# CAPE YORK IIIAB IRON METEORITE: TRACE ELEMENT DISTRIBUTION IN MINERAL AND METALLIC PHASES

Christian KOEBERL, Helmut H. WEINKE, Friedrich KLUGER† and Wolfgang KIESL

*Institute of Geochemistry, University of Vienna, P.O. Box 73, A-1094 Vienna, Austria*

***Abstract:*** Several mineral and metallic phases in a sample from the Agpalilik mass of the Cape York iron meteorite shower have been analysed for major and trace elements using electron microprobe analysis, rapid instrumental neutron activation analysis, instrumental neutron activation analysis, radiochemical neutron activation analysis, thermochemical methods, and secondary ion mass spectrometry. The phases investigated in this way included kamacite, plessite, taenite, troilite, chromite, and schreibersite. In addition, a rare nickel-rich phase has been found and is described in detail. The genetic implications of the presence of the nickel-rich phase (which may be termed nickel-rich taenite, but does not seem to be related to tetrataenite) are very important. A compositional gradient in Ni and Cu distribution is present, with the largest values near the troilite boundary and the lowest near the kamacite boundary. The phase occurs exclusively at the troilite/kamacite interface and is often associated with rhabdite. It seems as if this was one of the last precipitates from a very Ni-rich troilite-taenite liquid, after schreibersite crystallization purged the system for several siderophile elements. This is supported by the distribution of trace elements between troilite, kamacite, and schreibersite. A fractional crystallization history for the origin of Cape York, starting with dendrites, seems plausible.

## 1. Introduction

The Cape York iron meteorite is one of the most famous extraterrestrial samples found on earth. It constitutes probably the most massive shower ever recorded. Large masses totalling about 58 t have been recovered from the Melville Bay in Northwest Greenland. The shower fell presumably long before the region became inhabited by the Eskimos, who frequently used the iron for manufacturing some tools. It was from these tools that early in the 19th century several explorers concluded about the existence of a large meteoritic mass in the area. The story of the recovery of the samples is summarized very impressively by BUCHWALD (1975).

One of the best analysed samples is the 20 t mass of Agpalilik, which was transferred to Copenhagen in 1967. Some samples are covered with shallow pits and depressions, some of which resemble regmaglypts. Some outer parts show heat-affected $\alpha_2$-zones containing micromelted phosphides. A medium Widmanstätten structure of long lamellae (about 1.2 mm wide), sometimes with taenite included in

† Deceased January 27, 1986.

the kamacite lamellae is found frequently. Neumann bands are common and sometimes distorted. Taenite and plessite (Fe(Ni)) are fairly common, occurring as isolated taenite ribbons, as comb and net plessite and as small wedges of martensitic plessite. Schreibersite ($(Fe, Ni)_3P$) is common at grain boundaries but not as skeleton crystals. Some of the smaller phosphides are attached to the taenite. Rhabdites are frequently encountered, decorating subboundaries of kamacite lamellae. Troilite (FeS) is very common in the form of nodules and Reichenbach lamellae (which also contain chromite and schreibersite). Large sections cut from the Agpalilik mass reveal an average troilite content of about 5.6 vol% for the whole meteorite.

The troilite contains several accessory minerals, some which are exsolution products, like daubreelite ($FeCr_2S_4$), and some which are undissolvable in troilite, like chromite ($FeCr_2O_4$). A more exhaustive general description is given by BUCHWALD (1975).

Several accessory minerals which are present in small quantities have been found in the Cape York meteorite in recent studies. BUCHWALD and SCOTT (1971) described carlsbergite (CrN) in the metal phase, while OLSEN *et al.* (1977) report the discovery of buchwaldite ($NaCaPO_4$). A thorough study of accessory minerals has been performed by KRACHER *et al.* (1977), who report the presence and the chemistry of four different phosphates ($Na_4Ca_3(Fe, Mg)(PO_4)_4$, $NaFePO_4$, $Na_4Mn(PO_4)_2$, and one unknown phosphate), djerfisherite ($K_3(Fe, Ni, Cu)_{13}(S, Cl)_{14}$), sphalerite ((Zn, Fe)S), ferroan-alabandite ((Mn, Fe)S), a K-bearing sulfide ($K_3(Fe, Ni, Cu)_{13}S_{14}$, silica, and copper. Some of these minerals and also chalcopyrrhotite ((Fe, Cu)S) have been reported also by RAMDOHR (1973), although the occurrence of this mineral is not undisputed (BUCHWALD, 1977). The previous chemical studies will be discussed later.

## 2. Experimental

### *2.1. Sample description*

A rectangular slab cut from the Agpalilik mass of the meteorite (specimen No. 153) was available for our studies. This sample contained a large troilite nodule, which was used in microprobe studies and subjected to radiochemical neutron activation analysis. Several other accessory minerals (such as chromite) were found previously during microscopic investigations. The rim of the troilite nodule was investigated in different layers for several mineral phases.

### *2.2. Microprobe studies*

Electron microprobe studies were carried out using a fully automated ARL-SEMQ electron microprobe with an energy dispersive system and five crystal spectrometers. Analyses were performed at an acceleration voltage of 20 keV (metal) and 15 keV (troilite) and a sample current of 20 nA. Since we had not analysed any decomposing phases such as alkali phosphates, no other conditions were used. Automatic on-line corrections were used for drift, background etc. Evaluation was subsequently performed using a program (WEINKE *et al.*, 1974) based on ZAF-correction processes. In any case all data reported are averages from a large number of single points.

*2.3. Instrumental Neutron Activation Analysis*

Two different methods of instrumental neutron activation analysis have been used, one being the usual technique (a short and a long-time irradiation with subsequent measuring cycles). The other technique is known as RINAA (Rapid Instrumental Neutron Activation Analysis) (KOEBERL and GRASS, 1983). For this purpose we used the very fast pneumatic transport and irradiation system which was installed at the Vienna Nuclear Research Center (Atominstitut der österreichischen Universitäten) some years ago. An early version of this system (which can also be used with the reactor in the pulsed mode, for which neutron fluxes of $10^{17}$ n cm$^{-2}$ s$^{-1}$ can be reached for a very short time) and its application for meteorite studies was described by KIESL (1971).

Since then the system has been upgraded, allowing samples to be transferred from the irradiation facility at the reactor core with very high transfer speed to the measuring chamber in 15 ms. The whole system is computer controlled, allowing to preprogram irradiation times and measuring cycles. Three detectors were used simultaneously: a Ge(Li)-detector, a NaI-detector, and a Cerenkov-detector for $\beta$-emitters. The Ge(Li) signals were fed into a preamplifier modified for high count rate operation. A crucial point of the other part of signal processing is the so-called loss free counting system in the virtual pulse generator version. This system has considerable advantages compared to conventional setups (classical pulse generator correction of dead-time losses) and is particularly well suited for the real-time correction of counting losses (WESTPHAL, 1981). Fast data acquisition (via a DMA processor) and evaluation of the spectra is fully computer controlled. One of the elements determined this way was rhodium, which is only rarely analysed. RINAA analyses using $^{104}$Rh (half-life 42 s, 556 keV) provide fast and reliable results. Several aspects of the construction, outline, data processing, etc., of the RINNA system in Vienna are discussed by SALAHI and GRASS (1981), HEDRICH and GRASS (1981), SCHINDLER (1981), POPP (1981), and KOEBERL *et al.* (1984).

*2.4. Radiochemical Neutron Activation Analysis*

Activation of the samples was carried out at the ASTRA reactor of the Seibersdorf research center for four days at a neutron flux of about $7\times10^{13}$ n cm$^{-2}$ s$^{-1}$. The samples were processed following a short cooling period using radiochemical techniques. The separation of the trace elements from the matrix and from each other was performed using mainly distillation (*e.g.* halide distillation), ion exchange, and solvent extraction methods. The separation techniques applied here follow parts of the methods described by KIESL *et al.* (1967), SCHAUDY *et al.* (1967, 1968), BAUER and SCHAUDY (1970), HERMANN *et al.* (1971), SEITNER *et al.* (1971), and KIESL (1971).

*2.5. Secondary Ion Mass Spectrometry*

The distribution of trace elements in coexisting phases in the Cape York meteorite was studied with Secondary Ion Mass Spectrometry (SIMS). The investigations were performed using a CAMECA IMS-300 ion probe at the Department of Chemistry, University of Antwerp, Belgium. The procedure involved bombarding the polished sections with a $^{16}O^+$ beam at an angle of 45°, separation of the positive secondary ions

(magnetically and electrostatically), and detection with an electron multiplier. The secondary ion currents measured had to be corrected by complicated calculations for mass coincidences resulting from oxides and hydrides of the main constituents and for isotopic abundances. Due to the limited mass resolution of the instrument, which resulted in peak overlaps at higher masses, only masses up to 71 were measured. The correction method uses the concept of the local thermal equilibrium (LTE) and several inner standards and is described in detail by WEINKE *et al.* (1979) and WEINKE (1980).

## 3. Results

The most important phases found in the meteorite have been studied in detail in respect of their major and trace element chemistry. Microprobe studies have been made of kamacite, plessite, taenite, troilite, and schreibersite. Most important was the discovery of a nickel-rich metallic phase. A similar phase has also been reported by ESBENSEN and BUCHWALD (1982). The maximum nickel concentration in the Ni-rich phase was 58.77 wt%. ESBENSEN and BUCHWALD (1982) record only a range (53–61 wt%) for the nickel-content in their Ni-rich phases. Consequently we have performed some studies on the distribution of several elements in the Ni-rich phase. Two different modes of occurrence for the Ni-rich phase have been encountered, a streched, lamellar form, and a dotted, eutectic form. The chemistry of both is the same. We have found that the lamellar form makes up most of the nickel-rich metal in the meteorite, occurring exclusively at the kamacite-troilite border. Average data for the nickel-rich phase and the other as obtained by microprobe studies are given in Table 1.

Phosphides were found to occur in different varieties, two of which are reported in Table 1. In addition, schreibersite and rhabdite (two phosphides of very different nickel content) are present in this meteorite, schreibersite being one of the phosphides reported here. Copper in the kamacite was below the limit of detection (about 100 ppm in this run), while in other phases sometimes rather high amounts of copper are present. An interesting case is the mineral "phosphide 1", which contains about 0.65% Cu. From element distribution pictures, however, we know that copper is usually distributed very inhomogeneously in almost all minerals. This is in accordance with the findings of KRACHER *et al.* (1975), who studied the distribution and chemistry of copper in meteorites. The nickel-rich phases were studied most intensely.

*Table 1. Major element data for the main phases in Cape York IIIAB iron, obtained by microprobe analysis. All data given here are averages from a large number of point analyses made at each phase. All data in wt %.*

| | Fe | Ni | Co | Cu | P |
|---|---|---|---|---|---|
| Kamacite | 92.33 | 6.96 | 0.57 | — | 0.12 |
| Plessite | 83.20 | 16.30 | 0.37 | 0.026 | 0.049 |
| Taenite | 65.55 | 33.95 | 0.18 | 0.176 | 0.029 |
| Ni-rich metal | 40.50 | 58.77 | 0.37 | 0.226 | — |
| Troilite | 65.45 | — | — | 0.046 | — |
| Schreibersite | 49.87 | 32.96 | 0.12 | 0.11 | 15.60 |
| Phosphide 1 | 56.82 | 28.42 | 0.19 | 0.65 | 12.71 |

The data given in Table 1 is the part with highest Ni-content encountered. Usually we can refer to the phase as a nickel-rich taenite, a name which was also proposed by ESBENSEN and BUCHWALD (1982). It is not clear if this phase has any relations to tetrataenite. We do not feel that our nickel-rich phase is an ordered phase like tetrataenite (50% Ni/50% Fe). Mössbauer studies of the taenite lamellae (ALBERTSEN *et al.*, 1978, 1980) and Conversion Electron Mössbauer (CEM) studies (CHRISTIANSEN *et al.*, 1983) have shown that the ordered taenite (tetrataenite) is present mainly in the outer regions of the taenite lamellae, while the disordered taenite (with about 25% Ni) is present mainly in the clouded and the inner parts of the lamellae. No such behaviour has been found with the present nickel-rich phase, which never occurs inside the kamacite, but exclusively at the kamacite-troilite interface.

A fine example for the nickel-rich phase is depicted in Figs. 1a–1h. This is an example of the lamellar version, and is accompanied by rhabdite. The SEM picture (Fig. 1a) shows the general outline of the phase, while the other (element) pictures and the microprobe analyses yielded the distribution of several elements. A rather unusual result was the discovery of a kamacite inclusion within the Ni-rich phase. The kamacite inclusion is completely surrounded by the nickel-rich phase, which is clear from the Ni-distribution picture. We are, however, not able to exclude completely the possibility that this kamacite inclusion is only a visual artifact of cutting, but this would have required an usually shaped growth pattern. Compared to kamacite, cobalt is distributed more inhomogeneously, but at lower abundances. There seems to be no difference in the chromium abundance between kamacite and the nickel-rich phase. The distribution of copper is very interesting and characteristic. It can be seen from the copper picture very clearly that there are some considerable enrichments present, possibly in the form of small (1–5 $\mu$m diameter) Cu-nodules. These enrichments do not occur within the Ni-rich phase (and also not within either kamacite, troilite or rhabdite), but exclusively at the phase boundaries of the Ni-rich phase. Some are rimming the kamacite inclusion, while others are abundant at the upper left part of the phase. A few are present also at the troilite-rhabdite boundary below the Ni-rich inclusion. It seems as if this area had a very interesting nucleation behaviour.

Further investigations have been made concerning the quantitative distribution of the elements within the inclusions. Several microprobe scans have been made across some of the Ni-rich inclusions to determine the distribution of Ni, Fe, and Cu (see Table 2). The scans have not been made across the inclusion depicted in Fig. 1 because of the kamacite inclusion (which may disturb the distribution picture; also this was the only kamacite inclusion detected in a Ni-rich phase).

Copper was included to check if there is a similarity to normal taenite. A plot of the three elements is given in Fig. 2. Here we see that the analogy with taenite ends already. Neither Ni nor Cu do show any of the characteristic taenite distributions (the so-called "M-distribution"). Instead, a rather steady concentration gradient was encountered, with the highest nickel abundances near the troilite and the lowest near the kamacite. Copper shows a similar distribution, iron the complimentary behaviour. The copper data plotted were checked not to include any of the copper nodules.

Trace elements have been determined via neutron activation analysis (RINAA, INAA, RNAA) in the metal, troilite, and schreibersite. The results together with

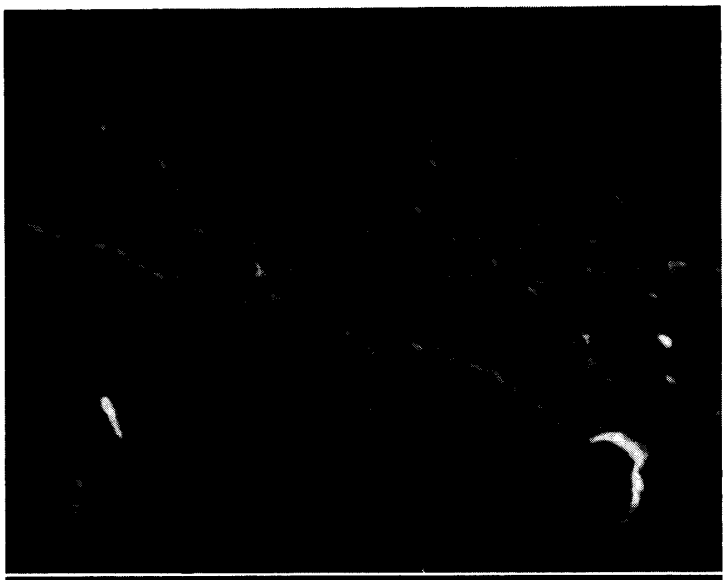

*Fig. 1a. SEM-picture of one of the Ni-rich inclusions which was found at the boundary between troilite and kamacite. The object at the lower right is of artificial origin. The width of the picture is 220 μm. The kamacite is rimmed by rhabdite.*

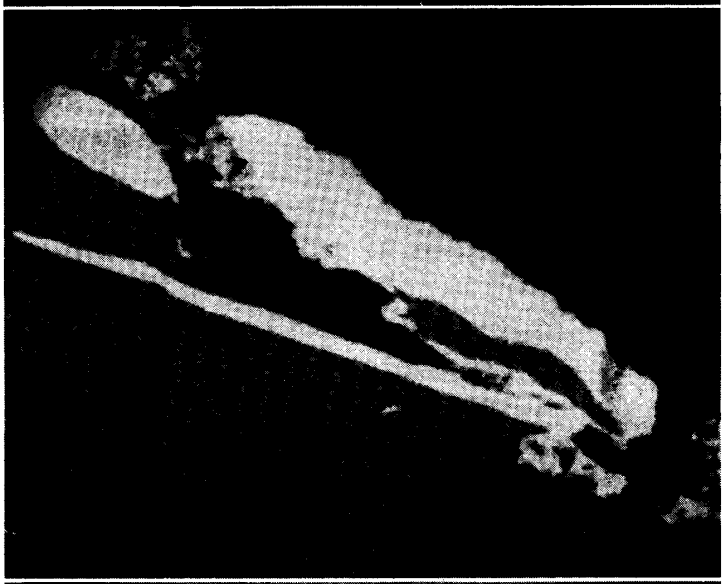

*Fig. 1b. Ni-distribution picture of the nickel-rich phase. Note the kamacite inclusion, which is completely surrounded by the Ni-rich metal. Also note the occurrence of small lumps of the (eutectic) Ni-rich phase at the top left of the picture, just above the elongated rhabdite nodule. This occurrence has lower nickel content.*

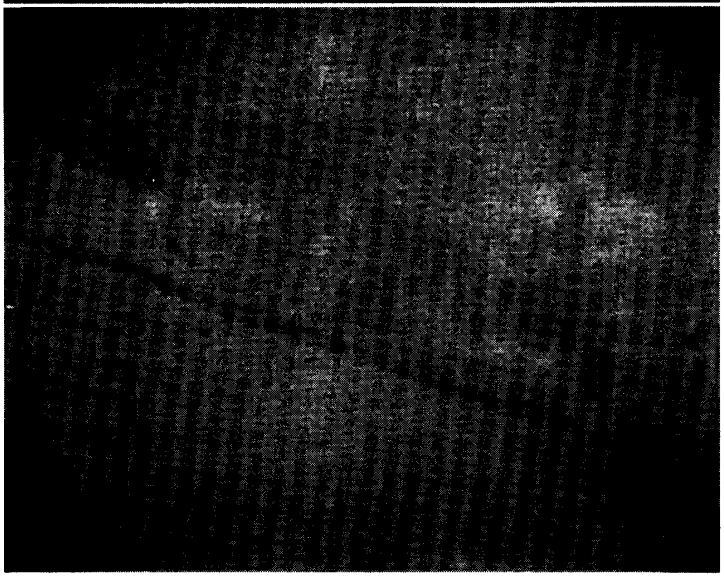

*Fig. 1c. Fe-distribution picture of the Ni-rich phase. The kamacite inclusion is clearly visible.*

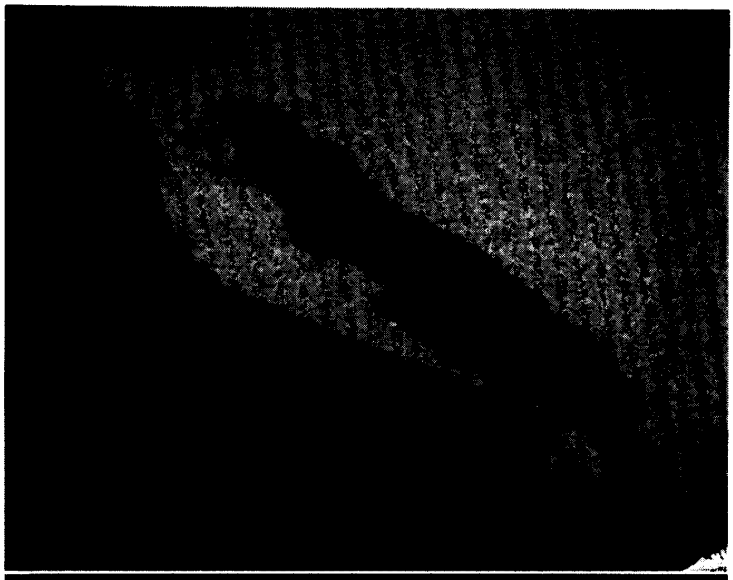

*Fig. 1d. S-distribution picture. The area in which the eutectic form of the Ni-rich phase occurs shows also a gradual depletion in sulphur.*

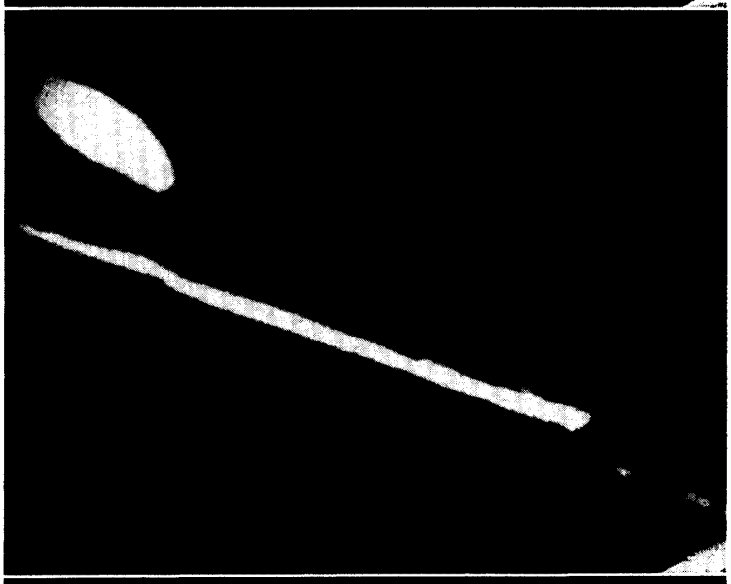

*Fig. 1e. P-distribution picture, clearly showing the distribution of rhabdite.*

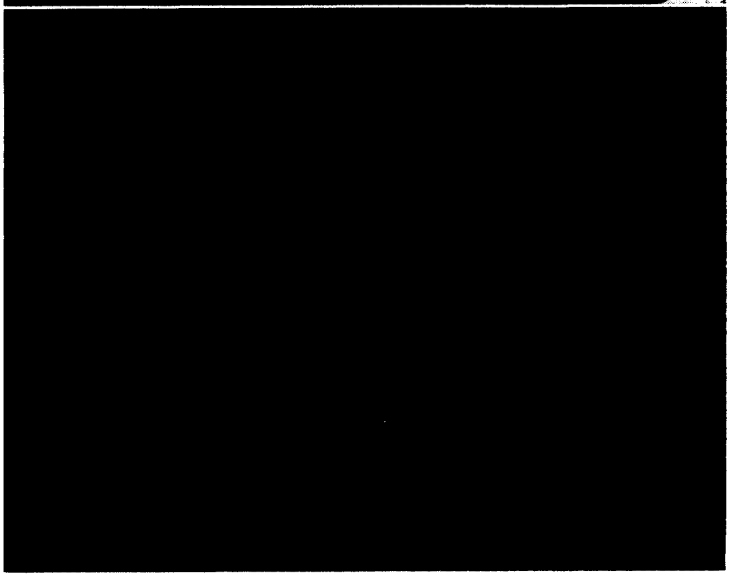

*Fig. 1f. Cr-distribution picture. Although Cr is a little bit lower than in the troilite, there seems to be no difference in the Cr-abundance in the kamacite and the Ni-rich phase.*

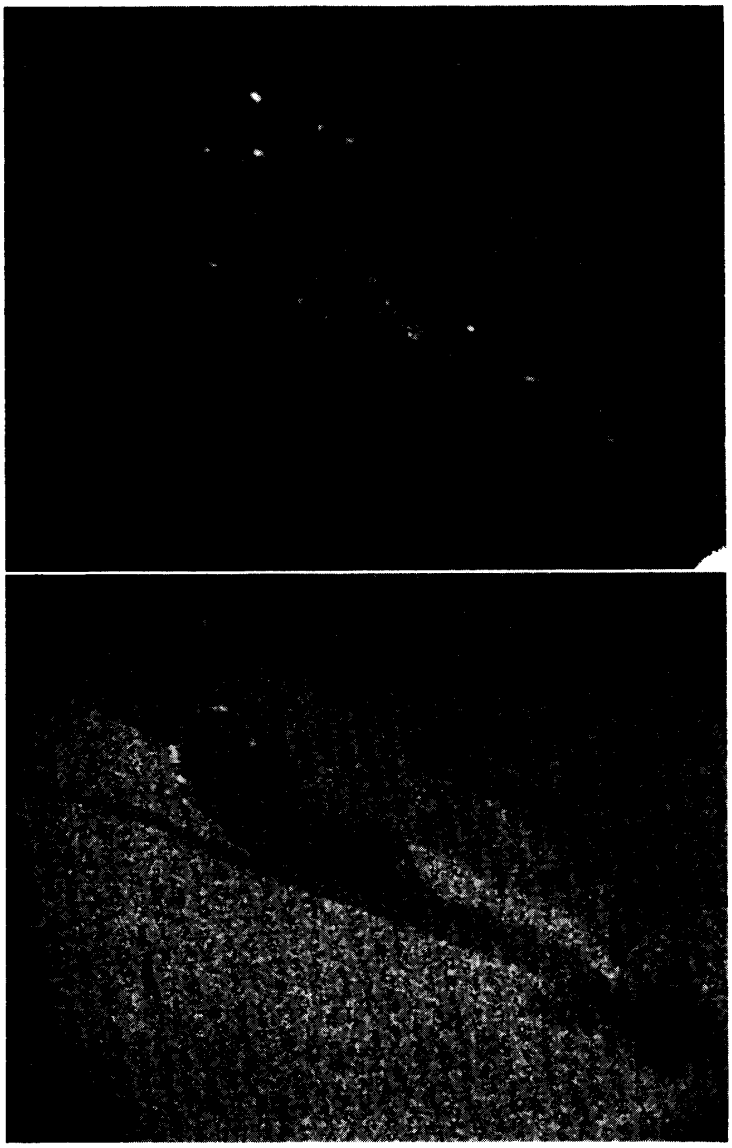

*Fig. 1g. Cu-distribution picture. Cu does not show any uniform distribution, although a good part of it is dissolved in the Ni-rich phase. An overall enrichment of copper in the Ni-rich phase compared to troilite or kamacite is visible. In addition, copper occurs in the form of copper nodules at the phase boundaries between the kamacite inclusion and the Ni-rich phase surrounding it as well as at the upper left part at the Ni-rich metal/troilite boundary. A few additional nodules occur at the rhabdite/troilite interface.*

*Fig. 1h. Co-distribution picture. The nickel-rich phase shows a lower overall cobalt abundance than the kamacite. The distribution is rather homogeneous. The Co-enrichments at the upper left may again be a hint for some special nucleation processes.*

carbon, nitrogen and sulphur data (obtained by thermoelectric/IR methods) are presented in Table 3. Some interesting results can be drawn from the data. Comparison with data from the literature (Table 4: metal, Table 5: troilite) shows a very good agreement. It is possible, however, that the agreement between different data sets is not perfect for natural reasons. ESBENSEN *et al.* (1982) have shown impressively that there are large variations of some elements (like Au, Ir, and Re) between the different masses of the Cape York meteorite, and that some elements show variations even within a single mass. They also demonstrated considerable variations within one troilite nodule, a result which was also obtained by JOCHUM *et al.* (1975).

Vanadium behaves as a chalcophile element when we compare metal and troilite (distribution ratio 0.016), but follows phosphorus (a siderophile element) even more prominently into schreibersite (distribution ratio 0.006). Several other elements show the same trend and seem to follow phosphorus very effectively. The vanadium content in the metal phase as obtained by SIMS analysis (see Table 6 for SIMS results)

*Table 2. Microprobe tracings across three different nickel-rich metal samples, present as inclusions at the phase boundary between troilite and kamacite. All tracings start near the troilite (distance in μm, 0 is at the phase boundary troilite/nickel-rich metal). Data in wt %.*

| Profile No. 1 | | | | Profile No. 2 | | | | Profile No. 3 | | | |
|---|---|---|---|---|---|---|---|---|---|---|---|
| Position μm | Cu | Ni | Fe | Position μm | Cu | Ni | Fe | Position μm | Cu | Ni | Fe |
| | wt % | | | | wt % | | | | wt % | | |
| 5 | 0.282 | 54.66 | 44.69 | 5 | 0.284 | 54.55 | 44.82 | 5 | 0.336 | 53.43 | 45.89 |
| 10 | 0.319 | 54.42 | 44.89 | 10 | 0.277 | 51.71 | 47.65 | 10 | 0.307 | 53.06 | 46.25 |
| 15 | 0.311 | 53.12 | 46.20 | 15 | 0.275 | 55.62 | 43.74 | 15 | 0.314 | 53.63 | 45.69 |
| 20 | 0.358 | 50.91 | 48.36 | 20 | 0.281 | 55.41 | 43.93 | 20 | 0.279 | 52.44 | 46.88 |
| 25 | 0.335 | 51.59 | 47.71 | 25 | 0.333 | 54.46 | 44.83 | 25 | 0.256 | 50.07 | 49.33 |
| 30 | 0.310 | 53.04 | 46.28 | 30 | 0.291 | 53.65 | 45.65 | 30 | 0.258 | 50.29 | 49.09 |
| 35 | 0.347 | 53.37 | 45.91 | 35 | 0.328 | 54.04 | 45.26 | 40 | 0.228 | 50.88 | 48.54 |
| 40 | 0.313 | 53.13 | 46.18 | 40 | 0.294 | 54.19 | 45.16 | 50 | 0.247 | 49.09 | 50.30 |
| 45 | 0.282 | 53.62 | 45.73 | 45 | 0.284 | 54.66 | 44.65 | 60 | 0.244 | 50.83 | 48.65 |
| 50 | 0.284 | 53.04 | 46.31 | 50 | 0.348 | 53.56 | 45.74 | 70 | 0.272 | 50.30 | 49.07 |
| 55 | 0.301 | 53.21 | 46.12 | 60 | 0.315 | 53.64 | 45.67 | 80 | 0.242 | 50.25 | 49.17 |
| 65 | 0.261 | 53.34 | 46.03 | 70 | 0.308 | 52.99 | 46.32 | 90 | 0.252 | 50.55 | 48.84 |
| 75 | 0.313 | 52.66 | 46.66 | 80 | 0.299 | 52.71 | 46.62 | 100 | 0.278 | 50.36 | 48.97 |
| 85 | 0.306 | 52.47 | 46.85 | 90 | 0.327 | 52.77 | 46.56 | 110 | 0.251 | 49.86 | 49.56 |
| 95 | 0.290 | 52.69 | 46.65 | 100 | 0.330 | 51.07 | 48.23 | 120 | 0.269 | 49.65 | 49.74 |
| 105 | 0.330 | 51.31 | 47.99 | 110 | 0.347 | 51.05 | 48.15 | 130 | 0.253 | 48.68 | 50.67 |
| 115 | 0.322 | 50.81 | 48.52 | 120 | 0.336 | 49.15 | 50.16 | 140 | 0.219 | 49.23 | 50.17 |
| 125 | 0.276 | 51.27 | 48.09 | 130 | 0.312 | 51.14 | 48.16 | 150 | 0.252 | 48.09 | 51.23 |
| 135 | 0.264 | 50.60 | 48.74 | 140 | 0.261 | 52.10 | 47.24 | 160 | 0.264 | 48.72 | 50.65 |
| 145 | 0.276 | 51.48 | 47.85 | 150 | 0.291 | 50.25 | 48.77 | 170 | 0.236 | 48.54 | 50.84 |
| 155 | 0.248 | 50.77 | 48.62 | 160 | 0.252 | 51.80 | 47.55 | 180 | 0.205 | 47.35 | 52.06 |
| 165 | 0.197 | 50.44 | 48.98 | 170 | 0.263 | 51.43 | 47.93 | | | | |
| 175 | 0.215 | 49.49 | 49.94 | 180 | 0.264 | 51.23 | 48.11 | | | | |
| 185 | 0.244 | 49.72 | 49.67 | 190 | 0.269 | 51.02 | 48.34 | | | | |
| 195 | 0.219 | 49.35 | 50.06 | 200 | 0.256 | 50.46 | 48.99 | | | | |
| 200 | 0.236 | 49.47 | 49.92 | 210 | 0.243 | 50.55 | 48.99 | | | | |
| 205 | 0.220 | 48.83 | 50.62 | 220 | 0.210 | 50.15 | 49.29 | | | | |
| 210 | 0.217 | 48.33 | 51.02 | 225 | 0.247 | 50.10 | 49.28 | | | | |
| | | | | 230 | 0.248 | 49.56 | 49.82 | | | | |
| | | | | 235 | 0.258 | 49.05 | 50.32 | | | | |
| | | | | 240 | 0.237 | 48.44 | 50.94 | | | | |
| | | | | 245 | 0.224 | 48.94 | 50.45 | | | | |

is higher than the NAA results by a considerable factor. At present we do not have an explanation for this. We feel, however, that the NAA data are more accurate.

The SIMS data are, in general, of lower accuracy than the comparable NAA data. In many cases, however, the agreement between SIMS data and NAA data and also with the literature data is rather good. Kamacite, plessite, and troilite have been analysed by SIMS at different positions. Since we know very little about inhomogeneities, this may be the cause for differences between the data. For example, a comparison with the troilite data of JOCHUM *et al.* (1975), who analysed different parts of a troilite nodule for trace elements using mass spectroscopy, shows that there are very important and large differences between the trace element contents in the different

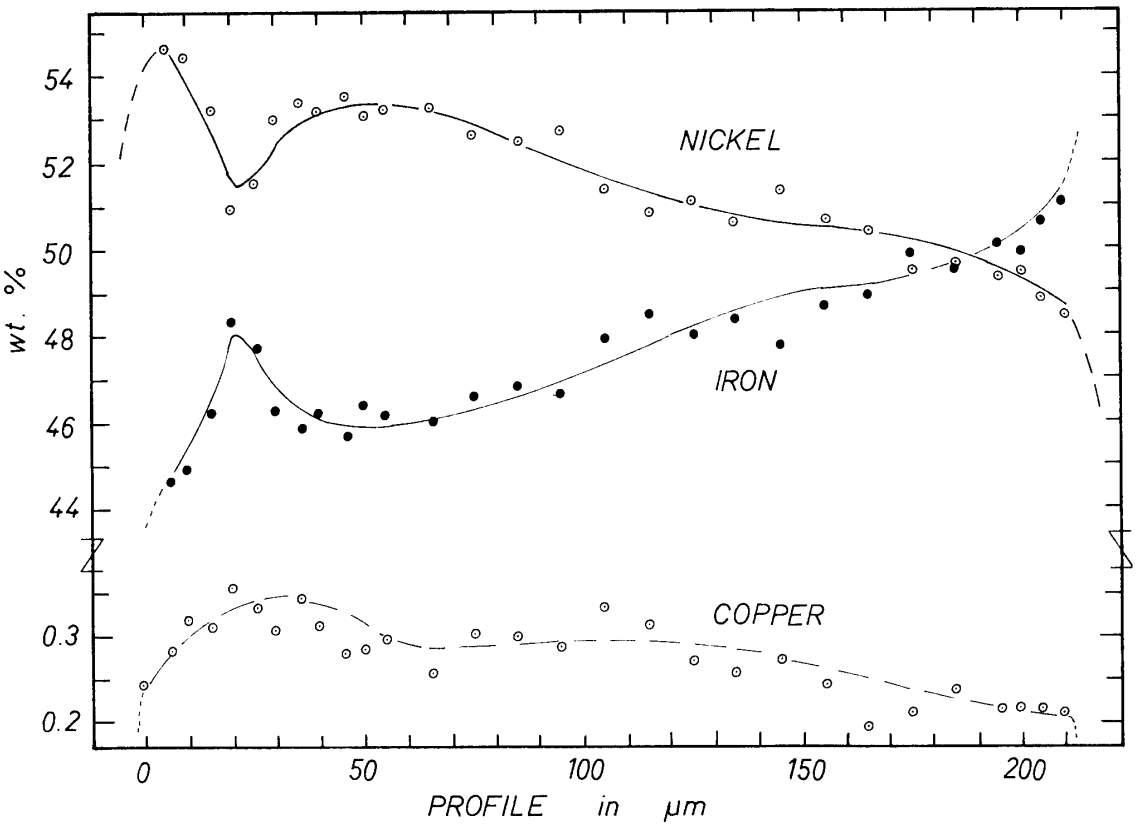


*Fig. 2. Microprobe tracing across one of the nickel-rich inclusions (for data see Table 2, column 1). A gradient is visible. The troilite is to the left, the kamacite to the right. Nickel has its highest abundance near the troilite and decreases towards the kamacite. Iron shows just the reverse behaviour. The distribution of copper does not follow one of the two other main constituents directly, but shows in general about the same behaviour as nickel. The overall abundance of copper is rather high compared to other phases.*

parts of the nodule. About the same effect is visible within the nodule we analysed (designated troilite (1) and (2)).

Chromites are found frequently within troilite nodules, preferentially on one side of the elongated nodules. Usually this one-sided concentration is attributed to formation in a gravitational field. An interesting example of a chromite inclusion is given in Figs. 3a–3d. A chromite crystal at the border of kamacite/troilite is shown, which itself includes a troilite inclusion. The most interesting pattern, however, is shown by the copper distribution. A dendritic growth pattern starting from the kamacite boundary is visible. This may have some important genetic consequences.

## 4. Discussion

The study of the Cape York meteorite, with its richness in inclusions, contributes a lot to our knowledge of the genetic history of the IIIAB parent body. The study of the inclusions, especially of the new Ni-rich phase, provided some insights in the development of this sample. ESBENSEN and BUCHWALD (1982) present a thorough discussion of the genetic significance of the Ni-rich phases. They show from con-

*Table 3. Trace element data for Cape York troilite, metal and phosphide (schreibersite), obtained by thermochemical, RINAA, INAA, and RNAA methods.*

| | Metal | Troilite | Phosphide |
|---|---|---|---|
| C | 83 ppm | n.d. | n.d. |
| N | 40 ppm | n.d. | n.d. |
| S | 15.3 ppm | n.d. | n.d. |
| Ti | <17 ppm | 24 ppm | <14 ppm |
| V | 0.06 ppm | 3.7 ppm | 9.9 ppm |
| Mn | n.d. | 200 ppm | n.d. |
| Co | 4800 ppm | 5.2 ppm | 1090 ppm |
| Ni | 7.71 wt % | n.d. | 32.6 wt % |
| Cu | 189 ppm | 110 ppm | 390 ppm |
| Zn | 1.50 ppm | 8.7 ppm | n.d. |
| Ga | 14.5 ppm | <1.5 ppm | 12 ppm |
| As | 6.1 ppm | 1.9 ppb | n.d. |
| Se | 5.5 ppb | 90.4 ppm | n.d. |
| Mo | 7.2 ppm | 5.6 ppm | n.d. |
| Ru | 4.5 ppm | 16 ppb | n.d. |
| Rh | 1.65 ppm | <0.2 ppm | 2.0 ppm |
| Re | 0.40 ppm | <0.4 ppb | n.d. |
| Os | 3.8 ppm | <5 ppb | n.d. |
| Ir | 4.60 ppm | 3 ppb | n.d. |
| Au | 1.4 ppm | 1.4 ppb | n.d. |

n.d.: not determined.

*Table 4. Trace elements in Cape York metal. Comparison data from the literature. All data in ppm, except Ni in wt %.*

| | 1 | 2 | 3 | 4 | 5 | 6 |
|---|---|---|---|---|---|---|
| C | | | | 430 | | |
| N | | | | | | 36.7 |
| P | | | | 1400 | | |
| S | | | | 60 | | |
| Cr | 51 | | | | | |
| Co | | | | 4800 | 5140 | |
| Ni | | 7.58 | 7.47 | 7.69 | 8.23 | |
| Cu | 163 | | | | 166 | |
| Zn | 4.2 | | | | | |
| Ga | 15 | 19.2 | 19.2 | | 19.9 | |
| Ge | 37 | 36 | 36 | | | |
| As | 3.5 | | | | 7.99 | |
| Mo | 6.0 | | | | | |
| Pd | 2.5 | | | | | |
| Ag | <0.01 | | | | | |
| In | <0.01 | | | | | |
| Sb | 0.28 | | | | | |
| W | | | | | 1.02 | |
| Re | | | | | 0.27 | |
| Ir | | 5.0 | 4.9 | | 2.73 | |
| Au | | | | | 0.97 | |

(1) SMALES *et al.* (1967), (2) SCOTT *et al.* (1973), (3) WASSON and KIMBERLIN (1967), (4) MOORE *et al.* (1969), (5) ESBENSEN *et al.* (1982), (6) PROMBO and CLAYTON (1983).

*Table 5. Comparison data for Cape York troilite, taken from JOCHUM et al. (1975). Data columns 1 and 2 are from two extreme ends of a large (ca. 7 cm) troilite nodule. All data in ppm, except where indicated.*

| | 1 | 2 | | 1 | 2 |
|---|---|---|---|---|---|
| Na | 2.1 | 2.1 | Ga | 12 | 0.20 |
| P | 4.0 | 0.90 | Ge | 0.19 | 0.094 |
| K | 2.8 | 3.4 | As | <0.01 | |
| V | 230 | 7.6 | Se | 92.0 | 38.0 |
| Cr (wt %) | 5.0 | 0.10 | Mo | 15.0 | 8.6 |
| Mn | 530 | 170 | W | <0.7 | |
| Co | 63 | 36 | Re | <0.5 | |
| Ni | 640 | 340 | Ir | <1.0 | |
| Cu | 470 | 50 | Pt | <0.8 | |
| Zn | 1340 | <19 | Au | <0.2 | |

*Table 6. Trace element abundances in Cape York kamacite, plessite, troilite, and chromite, obtained by SIMS (ion microprobe). All data in ppm, except as noted. Analyses are from different parts of the sample.*

| | Kamacite | | Plessite | | Troilite | | Chromite |
|---|---|---|---|---|---|---|---|
| | (1) | (2) | (1) | (2) | (1) | (2) | (1) |
| Na | <0.05 | <0.08 | <0.09 | <3 | <0.7 | <0.04 | <1.3 |
| Mg | — | 0.8 | <1 | <2 | <5 | <0.2 | 1260 |
| Al | 5 | 12 | 9 | 6 | 5 | 2 | 2.6 |
| Si | 19 | 34 | 56 | 56 | <51 | 11 | 57 |
| P | 580 | 1040 | <370 | <270 | <200 | <60 | <76 |
| K | <0.2 | <0.5 | <0.5 | <3 | <0.2 | <0.1 | <0.5 |
| Ca | 0.1 | 2 | 6 | 2 | 0.5 | 0.1 | 5.5 |
| Sc | <0.1 | <0.1 | <0.2 | — | <0.3 | <0.2 | <0.1 |
| Ti | <0.1 | <0.2 | <0.2 | <0.2 | <3 | <0.3 | 1.6 |
| V | 5 | — | — | 4 | 12 | 7 | 720 |
| Cr | 3 | 9 | 10 | 3 | 2870 | 940 | 41.54% |
| Mn | 20 | 20 | 12 | 19 | 2380 | 480 | 5120 |
| Co | 0.57% | 0.54% | 0.37% | 0.14% | <40 | 13 | 51 |
| Ni | | | | | <250 | <300 | <14 |
| Cu | 119 | — | 304 | 215 | 166 | 90 | 122 |
| Zn | <200 | <400 | <400 | <160 | — | 2600 | 3200 |
| Ga | 20 | — | 43 | 15 | 23 | — | — |

sideration of the phase diagrams that the schreibersite precipitates from the Fe-Ni-S-P liquid prior to the crystallization of the nickel rich phase (which they designate as Ni-rich taenite). This is fully supported by our studies. Very often the Ni-rich phase is separated from the kamacite by rhabdite lamellae, which show also a concentration gradient. The same concentration gradient (in Ni) is also present in the Ni-rich phase (see Fig. 2). This clearly is in favour of a crystallization gradient in the same direction. ESBENSEN and BUCHWALD (1982) further state that the remaining taenite-troilite eutectic carries elemental copper as a minor component. Our studies of the copper distribution at the nickel-rich phase are in favour of their model. Copper nodules occur only at the boundaries of the Ni-rich phase, and elemental copper

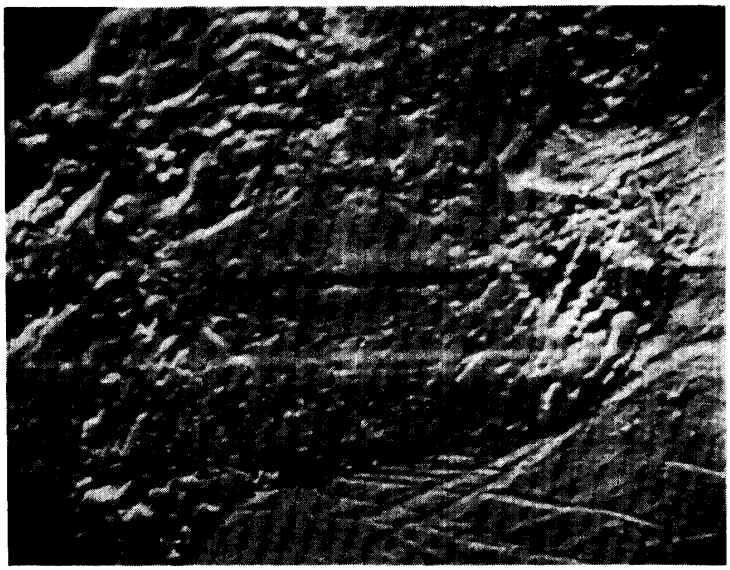

*Fig. 3a. SEM picture of a chromite found at the boundary kamacite/ troilite. Some elements in this unusual inclusion are shown in the other pictures. Width of the picture is 220 μm.*

shows a concentration gradient like Ni. The absence of considerable amounts of copper in the kamacite is also demonstrated by SIMS data. We found copper to be abundant in kamacite about three times less than in plessite. Data from CLARKE and JAROSEWICH (1978) show that Cu is enriched in taenite, but not observed in kamacite (their limit of detection is about 200–300 ppm, and thus consistent with our observation of about 100 ppm Cu in kamacite). They have found that copper in taenite behaves like Ni and depicts a M-shaped distribution. The overall abundance of Cu in the Ni-rich phase is much higher than in normal taenite, and does not show a M-pattern.

This is in accordance with a crystallization of the Ni-rich phase from a troilite-taenite eutectic as the last precipitate. The lamellar structure and the compositional zoning is explained in this way. The case of a kamacite inclusion within the nickel-rich inclusion can be explained by the possibility that the phase nucleated on the kamacite. The trace element partitioning between the troilite-taenite eutectic liquid and the kamacite took place long before the nucleation of the final precipitate (the nickel-rich taenite), leaving only the more chalcophile elements. This partitioning was not perfect, because of the high solubility of some of these elements at higher temperatures. Effective purging of the liquid for siderophile trace elements was most effective with the crystallization of the schreibersite.

Later in the crystallization history chromite formed. Between the solidification of the metal phase and the troilite there is a temperature interval of about 500°, in which the precipitation of the chromite took place. The occurrence of a troilite inclusion within a chromite inclusion complicates this simple picture. Since the chromite crystals are found almost exclusively on one end of the elongated nodules (and the one with the troilite inclusions is no exception), they must have sunk there in a troilite liquid due to a gravitational field. Either the cooling was so slow that a temperature gradient within the larger nodules formed, or some microscale remeltings occurred due to microchemical effects like heat of crystallization. We do not want to elaborate on the meaning of several trace element distributions in more depth until we have acquired

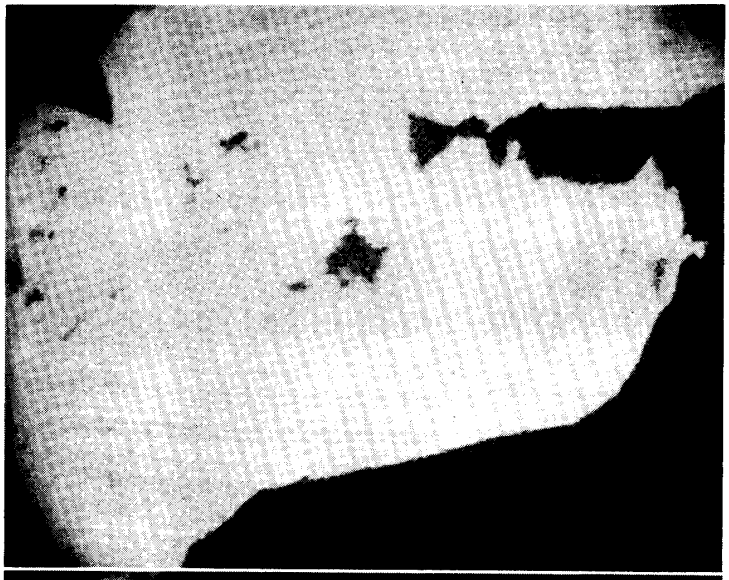

*Fig. 3b. Cr-distribution picture. Some "holes" are suspicious, and were shown in the sulphur picture to be troilite inclusions.*

*Fig. 3c. Sulphur distribution picture. It can be seen very clearly that there are troilite inclusions within the chromite inclusion (which is itself placed at the border of a large troilite nodule).*

*Fig. 3d. Cu-distribution picture. Copper shows a very interesting behaviour. The distribution is very inhomogenous, and the overall abundance is rather high. There is no copper visible in the troilite inclusions. Near the kamacite border a dendritic structure is visible.*

a more complete set of data. We do feel, however, that the differences in the distribution ratios for several siderophile trace elements between metal and troilite point to a very slow cooling history, allowing the distribution of these elements to be adjusted according to some physical differences between them. Indicative physical properties would be atom radii, migration coefficients, and volatility.

## 5. Summary and Conclusions

Several techniques (microprobe studies, rapid instrumental neutron activation, instrumental neutron activation, radiochemical neutron activation, thermochemical methods, and secondary ion mass spectrometry) have been used for the determination of the distribution of major and trace elements within a sample from the Agpalilik mass of the Cape York IIIAB iron meteorite. The most interesting discovery was a Ni-rich phase (described independently by ESBENSEN and BUCHWALD, 1982) occurring in two different varieties, a lamellar and a dotted (irregular) form. This phase contains more than 50% Ni and does not seem to show the ordered behaviour of tetrataenite. The distribution of some elements, measured with electron microprobe, is somehow similar to taenite, but without any M-shaped distribution and without the Agrell-effect. The compositional gradient present in these inclusions (high Ni and Cu near the border to the troilite and low concentrations of these elements near the border to kamacite) points to a crystallization gradient in the same direction. These inclusions could not have formed within a rapid-cooling melt. The associations of the Ni-rich phases with rhabdite and the sole occurrence at the kamacite-troilite interface supports the interpretation of these phase as one of the final precipitates in a Ni-rich troilite-taenite liquid. The liquid systems were presumably purged for siderophile elements by schreibersite/rhabdite since these phases have acquired a large fraction of the siderophiles present in the liquid, which is shown by the distribution coefficients of them between the metal and the minerals. Some elements show a fractionation behaviour between metal/troilite/phosphide or metal/troilite, which is not likely in quenched or rapid cooled melts (*e.g.* Mo, Ru, Ir, Au). The large-scale appearance of inclusions within sections of the Cape York mass are also not indicative of rapid cooling. Our investigations, together with the conclusions obtained by ESBENSEN and BUCHWALD (1982), are in favour of an origin of the Agpalilik mass by very slow cooling. Recent calculations of NARAYAN and GOLDSTEIN (1985) requiring fast cooling, are not supported by the obvious trace element distributions between the phases and the occurrence of a Ni-rich phase. A fractional crystallization model, starting with dendrites within a rather large parent body, seems most pertinently representing the data.

## Acknowledgements

We are grateful to our friend and coauthor F. K. for his dedication. He lost his battle against cancer on January 27, 1986, at age 46.

HHW likes to thank the colleagues at the University of Antwerp (Wilrijk, Belgium) for their hospitality, and help with their ion microprobe.

## References

ALBERTSEN, J. F., AYDIN, M. and KNUDSEN, J. M. (1978): Mössbauer effect studies of taenite lamellae of an iron meteorite Cape York (III-A). Phys. Scr., **17**, 467–472.

ALBERTSEN, J. F., KNUDSEN, J. M., ROY-POULSEN, N. O. and VISTISEN, L. (1980): Meteorites and thermodynamic equilibrium in f.c.c. iron-nickel alloys (25–50% Ni). Phys. Scr., **22**, 171–175.

BAUER, R. and SCHAUDY, R. (1970): Activation analytical determination of elements in meteorites 3. Chem. Geol., **6**, 119–131.

BUCHWALD, V. F. (1975): Handbook of Iron Meteorites. Vols. 1–3. Berkeley, Univ. California Press, 1418 p.

BUCHWALD, V. F. (1977): The mineralogy of iron meteorites. Philos. Trans. R. Soc. London, Ser. A, **286**, 453–491.

BUCHWALD, V. F. and SCOTT, E. R. D. (1971): First nitride (CrN) in iron meteorites. Nature, Phys. Sci., **233**, 113–114.

CHRISTIANSEN, A., LARSEN, L., ROY-POULSEN, H., ROY-POULSEN, N. O., VISTISEN, L. and KNUDSEN, J. M. (1983) The distribution of Fe-Ni phases in different layers of a taenite lamella from the iron meteorite Cape York—studied by combining Conversion Electron Mössbauer Spectroscopy and etching (abstract). Meteoritics, **18**, 281.

CLARKE, R. S., Jr. and JAROSEWICH, E. (1978): The concentration and distribution of Cu in meteoritic metal. Meteoritics, **13**, 418–420.

ESBENSEN, K. H. and BUCHWALD, V. F. (1982): Planet(oid) core crystallization and fractionation—evidence from the Agpalilik mass of the Cape York iron meteorite shower. Phys. Earth Planet. Inter., **29**, 218–232.

ESBENSEN, K. H., BUCHWALD, V. F., MALVIN, D. J. and WASSON, J. T. (1982): Systematic compositional variations in the Cape York iron meteorite. Geochim. Cosmochim. Acta, **46**, 1913–1920.

HEDRICH, E. and GRASS, F. (1981): Measurements of hard beta emitters by Cerenkov detector. J. Radioanal. Chem., **61**, 295–305.

HERMANN, F., KIESL, W., KLUGER, F. and HECHT, F. (1971): Neutronenaktivierungsanalytische Bestimmung einiger Spurenelemente in meteoritischen Phasen. Microchim. Acta, **1971**, 225–240.

JOCHUM, K. P., HINTENBERGER, H. and BUCHWALD, V. F. (1975): Distribution of minor and trace elements in the elongated troilite inclusions of the Cape York iron Agpalilik. Meteoritics, **10**, 419–422.

KIESL, W. (1971): On the determination of trace elements in meteoritic phases by neutron activation analysis. Activation Analysis in Geochemistry and Cosmochemistry, ed. by A. O. BRUNFELT and E. STEINNES. Oslo, Universitetsforlaget, 243–251.

KIESL, W., SEITNER, H., KLUGER, F. and HECHT, F. (1967): Determination of trace elements by chemical analysis and neutron activation in meteorites of the collection of the Viennese Museum of Natural History. Monatsh. Chem., **98**, 972–992.

KOEBERL, C. and GRASS, F. (1983): Rapid instrumental neutron activation analysis (RINAA); Application for tektite and impactite analysis. Meteoritics, **18**, 325–326.

KOEBERL, C., BERNER, R. and GRASS, F. (1984): Lithium in tektites and impact glasses; A discussion. Chem. Erde, **43**, 321–330.

KRACHER, A., MALISSA, H., WEINKE, H. H. and KIESL, W. (1975): Über die Zusammensetzung meteoritischen Kupfers. Microchim. Acta, **1975** (Suppl. 6), 251–256.

KRACHER, A., KURAT, G. and BUCHWALD, V. F. (1977): Cape York; The extraordinary mineralogy of an ordinary iron meteorite and its implication for the genesis of IIIAB irons. Geochem. J., **11**, 207–217.

MOORE, C. B., LEWIS, C. F. and NAVA, D. (1969): Superior analyses of iron meteorites. Meteorite Research, ed. by P. M. MILLMANN. Dordrecht, D. Reidel, 738–748.

NARAYAN, C. and GOLDSTEIN, J. I. (1985): A major revision of iron meteorite cooling rates—An

experimental study of the growth of the Widmanstätten pattern. Geochim. Cosmochim. Acta, **49**, 397–410.

OLSEN, E., ERLICHMANN, J., BUNCH, T. E. and MOORE, P. B. (1977): Bunchwaldite, a new meteoritic phosphate mineral. Am. Mineral., **62**, 362–364.

POPP, R. (1981): A fast event processor for counting loss-corrected gamma spectrometry. J. Radioanal. Chem., **61**, 361–366.

PROMBO, C. A. and CLAYTON, R. N. (1983): Nitrogen isotopes in iron meteorites. Meteoritics, **18**, 377–379.

RAMDOHR, P. (1973): The Opaque Minerals in Stony Meteorites. Amsterdam, Elsevier, 245 p.

SALAHI, A. and GRASS, F. (1981): A rapid transportation facility for irradiation with thermal and fast neutrons. J. Radioanal. Chem., **61**, 63–68.

SCHAUDY, R., KIESL, W. and HECHT, F. (1967): Activation analytical determination of elements in meteorites 1. Chem. Geol., **2**, 279–287.

SCHAUDY, R., KIESL, W. and HECHT, F. (1968): Activation analytical determination of elements in meteorites 2. Chem. Geol., **3**, 307–312.

SCHINDLER, P. (1981): An outline of the nuclear activation system at the Atominstitut. J. Radioanal. Chem., **61**, 307–311.

SCOTT, E. R. D., WASSON, J. T. and BUCHWALD, V. F. (1973): The chemical classification of iron meteorites—VII. A reinvestigation of irons with Ge concentrations between 25 and 80 ppm. Geochim. Cosmochim. Acta, **37**, 1957–1983.

SEITNER, H., KIESL, W., KLUGER, F. and HECHT, F. (1971): Wet chemical analysis and determination of trace elements by neutron activation in meteorites. J. Radioanal. Chem., **7**, 235–248.

SMALES, A. A., MAPPER, D. and FOUCHÉ, K. F. (1967): The distribution of some trace elements in iron meteorites, as determined by neutron activation. Geochim. Cosmochim. Acta, **31**, 673–720.

WASSON, J. T. and KIMBERLIN, J. (1967): The chemical classification of iron meteorites—II. Irons and pallasites with germanium concentrations between 8 and 100 ppm. Geochim. Cosmochim. Acta, **31**, 2065–2093.

WEINKE, H. H. (1980): Korrekturverfahren in der quantitativen Ionenstrahlmikroanalyse. Mitt. Österr. Mineral. Ges., **1980**, 33–41.

WEINKE, H. H., MALISSA JUN., H., KLUGER, F. and KIESL, W. (1974): Korrekturprogramm für quantitative Elektronenstrahlmikroanalyse. Microchim. Acta, **1974** (Suppl. 5), 233–256.

WEINKE, H. H., KIESL, W. and GIJBELS, R. (1979): Untersuchungen an meteoritischem Eisen mit der Ionensonde. Microchim. Acta, **1979** (Suppl. 8), 87–95.

WESTPHAL, G. P. (1981): High rate gamma spectroscopy and related problems. J. Radioanal. Chem., **61**, 111–119.

*(Received July 5, 1985; Revised manuscript received November 9, 1985)*